The Tubulin-Bound Conformation of Discodermolide Derived by NMR Studies in Solution Supports a Common Pharmacophore Model for Epothilone and Discodermolide**

*Víctor M. Sánchez-Pedregal, Karel Kubicek, Jens Meiler, Isabelle Lyothier, Ian Paterson, and Teresa Carlomagno**

Discodermolide (DDM) is an antimitotic polyketide, isolated from a deep-sea sponge, that displays potent cytotoxic activity against a number of human tumor cell lines.[1–3] In a similar manner to taxol and epothilone (EPO), DDM suppresses normal microtubule (MT) dynamics and disrupts the formation of mitotic spindles, thus leading to apoptosis.[4–6] DDM binds to tubulin more strongly than taxol, is more efficient in promoting tubulin polymerization, and is active also in taxol-resistant ovarian and colon carcinoma cells.[1] These properties have triggered strong interest in DDM as a lead structure for the development of a novel cancer chemotherapeutic agent. Competition experiments with radiolabeled taxol show that DDM displaces taxol from tubulin, thereby suggesting an overlapping binding site for the two drugs.[7] However, an allosteric mechanism as a basis for the competitive binding of taxol and DDM to tubulin cannot be ruled out.

The taxol binding site of tubulin can accommodate a variety of ligands, including epothilones, dictyostatin, and

[*] Dr. V. M. Sánchez-Pedregal,[+] Dr. K. Kubicek, Dr. T. Carlomagno
Abteilung NMR-basierte Strukturbiologie
Max-Planck-Institut für biophysikalische Chemie
Am Fassberg 11, 37077 Göttingen (Germany)
Fax: (+49) 551-201-2202
E-mail: taco@nmr.mpibpc.mpg.de

Prof. J. Meiler
Center for Structural Biology
Vanderbilt University
654 21st Ave South, BIOSCI/MRBIII, Nashville, TN 37212 (USA)

Dr. I. Lyothier, Prof. I. Paterson
Department of Chemistry
University of Cambridge
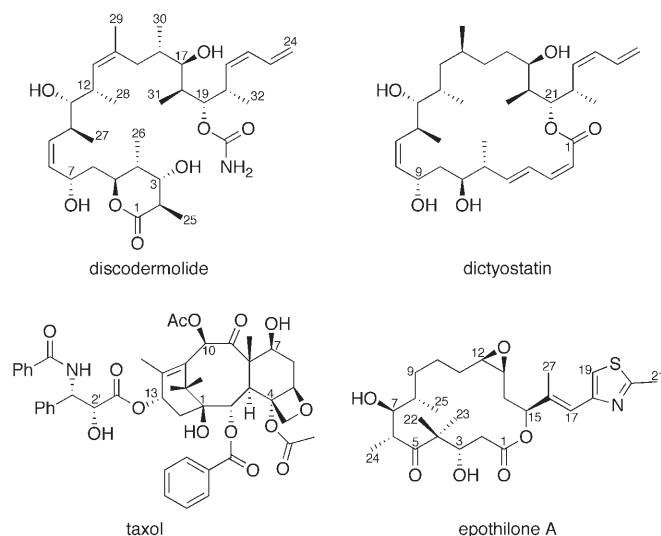Lensfield Road, Cambridge, CB21EW (UK)

[+] Present address: Facultad de Química
Dpto. Química Orgánica
Universidad de Santiago de Compostela
Campus Universitario Sur, s/n
15782 Santiago de Compostela (Spain)

Supporting information for this article is available on the WWW under http://www.angewandte.org or from the author.

DDM, as well as others that share the MT-stabilizing activity of taxol while having very different chemical structures[8] (Scheme 1). Despite the availability of an impressive amount of structure–activity data, as well as modeling and

29 30
17 OH 24
HO,,, 12 28 31 19 ,,,32
27 26 O O
7 3 OH NH$_2$
OH O
O

discodermolide

OH
HO,,, 21 ,,,
9 O O
OH OH

dictyostatin

Ph NH O AcO O OH
13 10 7
Ph 2' 1 4 O
OH HO O H O
O O

taxol

12 O
O 27 19 S
9 25 15 17 21
HO 7 22 23 N
24 5 3 1 O
O OH O

epothilone A

Scheme 1. Structures of discodermolide, dictyostatin, taxol, and epothilone A.

structural studies,[9] an explanation of how different classes of structurally unrelated molecules exert a similar effect on MT dynamics is still lacking. Direct structural information on the interaction of these natural products with tubulin is limited to the complexes of tubulin either with taxol or epothilone A (EPO-A), as determined by electron diffraction studies of Zn-stabilized two-dimensional sheets of tubulin.[10,11] In addition, we have determined the first tubulin-bound conformation of EPO-A in the solution state by NMR spectroscopy[12] by using a combination of transferred NOE (tr-NOE) and transferred cross-correlated relaxation data.[13] As for DDM, the free conformation of the molecule has been determined in solution by NMR spectroscopy[14,15] and in the solid state by X-ray diffraction,[16] while its tubulin-bound structure has remained elusive.

Herein, we derive for the first time the bioactive, tubulin-bound conformation of DDM in solution by NMR structural analysis. Additionally, we apply the recently developed INPHARMA technique,[17] which is based on the observation of protein-mediated interligand NOE signals, to prove that DDM does indeed bind to the taxane binding pocket and this, in turn, enables a common pharmacophore model for EPO and DDM to be constructed.

NOESY spectra of tubulin-free DDM show weak cross-peaks, as expected for a small molecule tumbling rapidly in solution. In contrast, the NOESY spectra of a solution of 500 μM DDM in the presence of 10 μM tubulin show intense cross-peaks (tr-NOE), thus indicating that DDM binds to soluble tubulin with $k_{off} > 100$ Hz, as previously shown for EPO-A.[12] The NMR sample is devoid of GTP and Mg^{2+} ions and contains instead 1.5 mM Ca^{2+} ions, which prevents complete polymerization of tubulin upon addition of

DDM.[18] Under these conditions DDM promotes polymerization of tubulin to form "microtubule sheets" or "open microtubules" (see the Supporting Information), which have been previously observed in MT preparations stabilized by EPO or taxol[19] and by GMPCPP at low temperature.[20] While it is known that DDM binds much tighter to MTs than to soluble tubulin, our data demonstrate that the weaker binding of DDM to soluble tubulin is functionally relevant as it triggers formation of ordered tubulin polymers, even in the presence of Ca^{2+} ions. Once the polymers are formed (see the Supporting Information), they precipitate out of solution in a few hours and do not contribute to the NMR signal. Our structural data correspond to DDM bound to soluble tubulin, namely to the first step in the chain of conformational change events that lead to the drug-induced formation of MTs. The binding constant of DDM to tubulin is larger than that of EPO-A, as derived by comparison of the intensity of tr-NOE signals at a short mixing time. The relative affinity of the different MT-stabilizing agents for soluble tubulin follows the same order as for their binding to preformed MTs,[21] further confirming the biological relevance of the interaction of the ligands with tubulin before polymerization.

A total of 201 nonredundant tr-NOE peaks were identified in the NOESY spectra and were used as restraints in the structure calculation. The complete relaxation matrix approach was used to calculate the structure of tubulin-bound DDM.[22] This method minimizes the difference between the computed and the experimental 2D NOE intensities while accounting for spin diffusion effects.

The structure calculations converged to a unique family comprising the 12 lowest energy conformers (Figure 1 A). The overall shape of the tubulin-bound DDM resembles that of free DDM in the solid state (Figure 1 B). In contrast, free DDM exists in DMSO solution as a family of over 10 different conformations,[15] none of which is as compact as that observed in the X-ray structure.[16]

While most natural products binding to tubulin in the taxane binding site can be roughly described as a combination of a central cyclic core and a side-chain tail,[23] DDM is a potentially more flexible linear molecule that does not fit into this body–tail description. However, our study demonstrates that, when bound to tubulin, the main carbon chain of DDM folds in a right-handed helical twist, thereby forming a central core that mimics the rigid cyclic skeleton of taxol or EPO. Such a fold was proposed in a computational DFT study conducted in the gas phase,[24] in which DDM was assumed to fit the body–tail structural motif by folding in the compact globular X-ray conformation.

The similarity between the tubulin-bound conformation of DDM and the X-ray structure provides a rationale for the potent biological activity of the marine natural product dictyostatin, a 22-membered macrocyclic lactone which is structurally and biogenetically related to DDM. Dictyostatin competes with the taxanes for tubulin binding and has an analogous effect on MT dynamics, which suggests that it interacts with tubulin in a similar way as DDM.[25] Not surprisingly, the tubulin-bound conformation of DDM derived here is closely related to the solution structure of dictyostatin in water (Figure 2), which supports a common
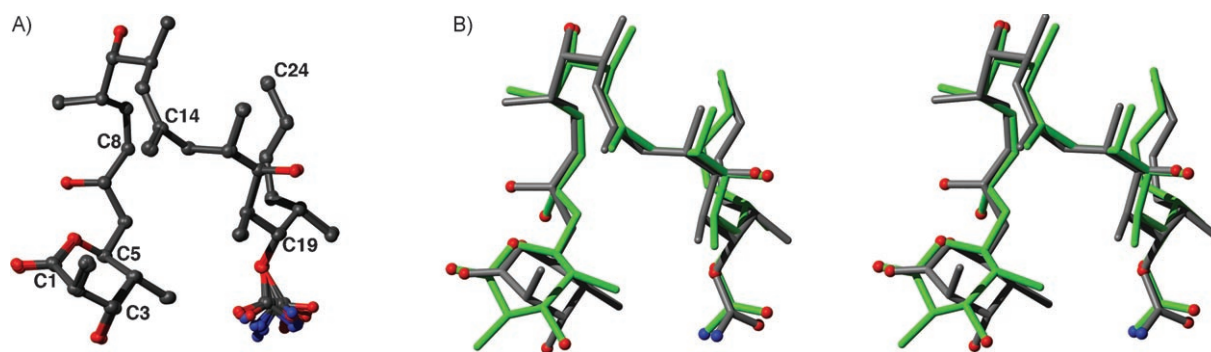
Figure 1. A) Superposition of the 12 lowest energy structures of DDM derived from NMR data (C gray, O red, N blue). The NMR-derived structure is well defined with a heavy-atom rmsd of 0.26 Å. B) Stereoview of the overlaid tubulin-bound (NMR-derived, in gray) and free (X-ray derived, in green)[16] conformations of discodermolide. Heteroatoms are displayed as spheres: O in red and N in blue. The two conformations are quite similar except for the lactone moiety. All figures were prepared with the program Molmol.[37]

Figure 2. Overlay of the tubulin-bound (NMR-derived, in gray) conformation of discodermolide and the solution conformation of free dictyostatin (in magenta).[25] Heteroatoms are displayed as spheres: O red and N blue.

mechanism for the MT-stabilizing activity of the two compounds.

The presence of strong structural requirements for the stability of the tubulin-bound compact helical conformation of DDM in the C6–C16 region is confirmed by the structure–activity relationship (SAR) data, which show that modifications in this segment are usually detrimental for activity. In particular, constraint of the C9–C13 section in a cyclopentane ring,[26] saturation,[27] or a change in the geometry of the C8–C9 or the C13–C14 double bonds from *Z* to *E*,[7,28] or inversion of the C16 configuration[29] severely affect the capacity of DDM to stabilize MTs.

The δ-lactone ring adopts a twisted-boat conformation in the solid-state structure, where all the substituents show a pseudoequatorial orientation that minimizes their nonbonding interactions. In contrast, the tubulin-bound conformation of the lactone is closer to a flattened chair, with two

substituents (2-Me and 3-OH) in an axial position and the other two (4-Me and the C5 main chain) adopting an equatorial position (Figure 1). The structural analysis of free DDM in DMSO solution shows both the boat and the chair conformations. Moreover, the torsion angles around the C5–C6 and C6–C7 bonds in the tubulin-bound structure differ from those in the X-ray structure by −43° and +19°, respectively. The conformational change occurring upon binding tubulin brings about a displacement of the position of the methyl group at C2 by 3.6 Å, while the position of the carbonyl group at C1 remains almost unvaried.

Several SAR studies show that the precise structural details of the lactone segment influence the activity only moderately. For example, simplification of the lactone ring (for example, by removal or inversion of the configuration at either one, two, or three of the substituents on C2–C4, or by reducing the size of the ring) leads to compounds with similar potency as the parent DDM (within one order of magnitude), thus indicating that the 3-hydroxy and the 2- and 4-methyl substituents do not play a critical role in determining DDM cytotoxicity.[27,30] However, the change in the conformation of the lactone observed upon tubulin binding places the methyl group at C2 close to the hydrophobic central body of DDM and is likely to be dictated by the need to optimize the contacts of the ligand with the hydrophobic floor of the protein binding pocket. Additionally, the significance of the configuration of butyrolactone analogues at C4[30] and the conspicuous loss in activity (one to three orders of magnitude) of DDM analogues in which the conformationally constrained lactone moiety has been replaced by diverse flexible esters or by substituted phenyl rings[31,32] underlie the relevance of the carbonyl group at C1 for activity. In agreement with this SAR data, the carbonyl group at C1 points away from the hydrophobic DDM skeleton, where it is readily available for contacts with hydrophilic protein side chains.

The one-dimensional ¹H and NOESY spectra showed that the δ-lactone ring of DDM opens up slowly by hydrolysis in the buffer. Comparison of the intensities of cross- and diagonal peaks reveals that the NOE rates of hydrolyzed DDM are only 15% of the NOE rates of intact DDM, thus indicating that binding of hydrolyzed DDM to tubulin is much weaker. This finding is in good agreement with activity data

showing that the potency of DDM decreases approximately by a factor of six upon opening of the lactone.[27]

We have recently developed a new methodology, called INPHARMA, which is based on the observation of protein-mediated interligand NOE signals and allows the definition of the relative binding mode of two ligands binding to a common target in a mutually exclusive manner.[17] Briefly, during the mixing time of a NOESY experiment, acquired on a mixture of two competitive ligands A and B and a receptor protein T, the binding pocket of T is occupied by either of the two ligands A and B. Spin-diffusion through protons of the receptor generates a set of intermolecular cross-peaks between those protons of ligands A and B that are close to a common receptor site in the TA and TB complexes. A number of such intermolecular NOE signals define the relative orientation of the two ligands.

We have now applied the INPHARMA methodology to a mixture of tubulin (12 µM), epothilone (500 µM), and disco-dermolide (70 µM) with the goal of determining a common pharmacophore for the two drugs. A number of interligand NOE signals are observed between the two ligands (Figure 3 A). Such NOE signals are not observed in the absence of the protein, thus confirming that they do not originate from the transient aggregation of the two ligands. Simultaneous binding of the two ligands to the protein can be excluded on the basis of biochemical data, thereby indicating that both DDM and EPO compete with taxol for tubulin binding.[1] The presence of protein-mediated interligand NOE signals verifies that DDM and EPO-A bind to the same binding pocket on tubulin, thus excluding an allosteric mechanism for the competitive binding of the two drugs. A summary of the observed interligand NOE signals is given in Figure 3 B.

The higher affinity of DDM for tubulin meant that we had to use a very low concentration of DDM (70 µM), with the consequence that the interligand NOE signals are rather weak and can be observed mostly for the intense resonances of the methyl groups. The extensive overlap of the resonances of EPO-A and DDM between $\delta = 1$ and 2.5 ppm does not permit interpretation of the interligand NOE signals in this region. Me25, Me28, and Me29 of DDM (Scheme 1 and Figure 3 B) show the strongest interligand NOE signals to both the side chain and ring protons of EPO, which indicates that these methyl groups are in contact with the protein surface. No interligand NOE signals can be evaluated for Me29 and Me32 of DDM because of the overlap with signals from Me25 and Me22 of EPO-A (Scheme 1).

As noted previously,[17] these protein-mediated interligand NOE signals can be quantitatively interpreted to discriminate between pairs of docking modes of the two ligands. However, the low intensity of the interligand NOE signals observed for the mixture of DDM and EPO-A in the presence of tubulin deterred us from a quantitative interpretation of the data. Instead, we assume that a partially overlapping pharmacophore exists for EPO-A and DDM, and we propose such a pharmacophore model guided by the qualitative interpretation of the interligand NOE signals and by the SAR data available for the two compounds. The presence of interligand NOE signals between one proton of DDM and one proton of EPO-A is interpreted as evidence
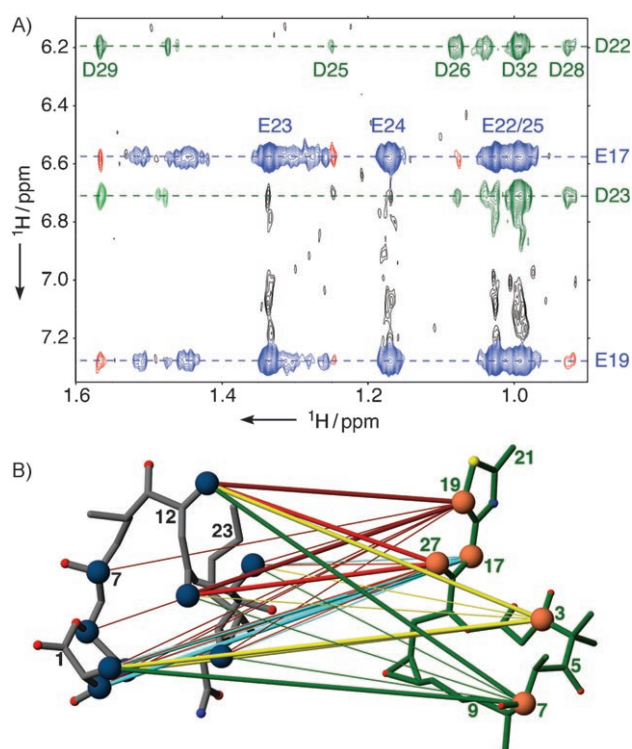

Figure 3. A) NOESY spectrum of the mixture DDM (70 µM), EPO-A (500 µM), and tubulin (12 µM) for the measurement of the INPHARMA NOE signals between the two ligands. The mixing time was 300 ms. Green and blue peaks represent intraligand transfer-NOE signals of DDM (labeled with D) and EPO-A (labeled with E), respectively, while the red peaks are the protein-mediated, interligand NOE signals (INPHARMA NOE signals). B) Schematic representation of the inter-ligand NOE signals observed between DDM and EPO-A. The carbon atoms carrying the protons that show interligand NOE signals between DDM and EPO-A in the presence of tubulin are represented as spheres (blue for DDM and orange for EPO-A). Lines connect the sites of the two molecules that show an interligand NOE signal. Thick and thin lines represent strong and weak interligand NOE signals, respectively. Interligand NOE signals to the protons H3, H7, H17, H19, and H27 of EPO-A are represented by yellow, green, blue, brown, and red lines, respectively.

that these two protons occupy close sites in their complexes with the protein. Additionally, our common pharmacophore model tries to match the regions of both DDM and EPO-A identified to be essential for the interaction with tubulin and to reproduce the position of H-bond acceptors/donors and of hydrophobic elements in the two molecules. However, we also consider that the different morphology of the micro-tubules obtained in the presence of DDM and EPO suggests nonfully overlapping pharmacophores for the two drugs.[1]

Similar to EPO, DDM has a disc shape with dimensions $11 \times 10 \times 4.5$ Å (Figure 4 A,B). The functional groups that are potentially involved in H bonds or in electrostatic interactions with the protein are concentrated on two edges of the disc, namely at the C1–C11 and at the C17–C19 regions (Figure 4 A). Similarly, the partially charged groups of EPO are concentrated on the N-C1-C5 side and at C7.[12] The interligand NOE data suggest that the thiazole side chain and the C1–C3 region of the macrolide ring of EPO-A are
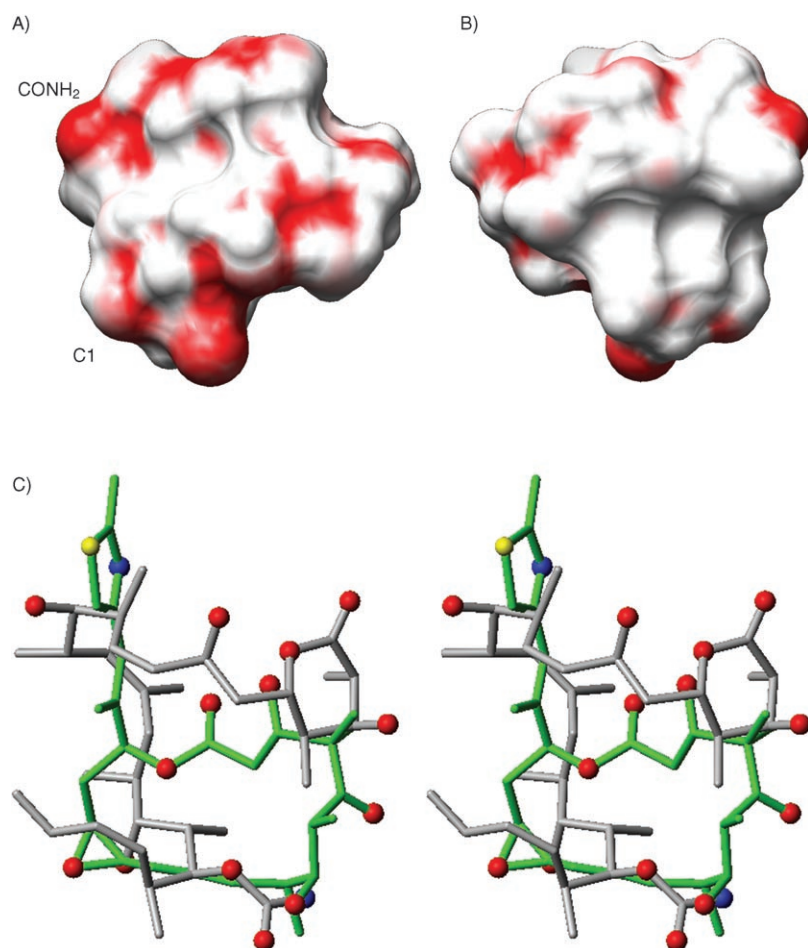
Figure 4. A) DDM, in a space-filling representation, has the form of a disc. The upper and lower edges present a high concentration of oxygen atoms (in red), while the flat sides of the disc are highly hydrophobic. B) Same as in (A) but turned 180° around the vertical axis. C) Stereoview of the common pharmacophore model for epothilone A (in green) and discodermolide (in gray) derived from INPHARMA NMR and literature SAR data. Heteroatoms are displayed as spheres: O red, S yellow, and N blue. In this model the C20–C24 tail of DDM is on the same side as the section C10–C13 of EPO-A, the carbamate group and the lactone ring occupy similar positions as the 7-OH group and C3−C4 unit of EPO-A, respectively, while the C8–C15 segment of DDM corresponds to the C15–C18 region of the side chain of EPO-A.

the sharp turn in the extended backbone and the two double bonds at C8−C9 and C13−C14. Both regions feature sites of unsaturation and can interact favorably with hydrophobic regions on the protein. However, DDM does not extend as far as EPO-A and lacks an aromatic ring. Fundamental differences in the interaction of the two ligands with the protein are anticipated in this region, which in the EPO-A/tubulin complex involves the key residue H227 of the tubulin helix H7.[11] These differences could account for the different morphology of the tubulin polymers stabilized by DDM and EPO.

The second hydroxy group in the macrolide ring of EPO-A, attached at C7, overlaps with the carbamate side chain of DDM (Figure 4C). It has been suggested that the 7-OH group of EPO is involved in contacts with tubulin side chains, as inversion of the configuration at C7 results in a considerable loss of potency.[33] Similarly, DDM analogues lacking the carbamate moiety at C19 have reduced MT-stabilizing activity, while most of the activity can be recovered by introduction of a carbamate group at C17 or an acetyl group at C19.[31] These data suggest that the presence of an H-bond acceptor is essential at similar positions in DDM and EPO.

Finally, the hydrophobic C20–C24 tail of DDM is situated on the same side as the C10–C13 hydrophobic section of EPO-A, but does not fully overlap with it. In our common pharmacophore model for DDM and EPO, the C20–C24 tail of DDM propagates from the C10−C11 bond of EPO towards the protein. Analogously to the C10–C13 segment in EPO-A, SAR data support the contact of the C20–C24 tail of DDM with a hydrophobic cleft of the tubulin binding pocket. In fact, substitution of the whole moiety with a number of lipophilic groups or reduction of one or both double bonds of the diene side chain is well tolerated,[34] while shortening of the segment to an isopropyl group or complete deletion has a detrimental effect on potency.[28] Similarly, the C10–C13 segment of EPO cannot be shortened without hampering the activity, while hydrophobic substituents on C12 even increase the potency. A previously proposed pharmacophore model suggests instead that the C20–C24 tail of DDM corresponds to the side chain of EPO-A.[35] This model, however, does not explain very well the intermolecular NOE signals observed between the side chain of EPO-A and the methyl groups of the C1–C11 stretch of DDM.

Two highly hydrophobic pockets are found in the taxane binding site of tubulin that could host the C20–C24 tail of DDM (see the Supporting Information): the first comprising A206, L207, and I210 of helix H6 as well as L228 of helix H7 (see the Supporting Information), and the second comprising the F270–P272 section of the M loop as well as A231 and G235 of helix H7 (see the Supporting Information). However, unlike taxol, DDM conserves full activity on cell lines presenting the F270V and A364T mutations,[1] which allows us to exclude the possibility that DDM closely interacts with the second pocket and to propose that the C20–C24 side chain

situated on the same side as the C1–C11 region of DDM, as we observe the strongest interligand NOE signals between Me25, Me28, and Me29 of DDM and H3, H19, and Me27 of EPO-A, while the interligand NOE signals of the same protons of EPO-A with Me30 and Me31 of DDM are weaker. Therefore, in our pharmacophore model the oxygen-rich C1–C11 region of DDM overlaps with the N-C1-C5 section of EPO-A (Figure 4C). The lactone ring of DDM, which is rich in hydrophilic groups, overlaps with the C3−C4 unit of EPO-A, with the O1 oxygen atom of DDM occupying a position close to the 3-OH group of EPO-A. The relevance of a hydrogen-bond acceptor in this region is supported by SAR data for both the carbonyl group at C1 of DDM and the 3-OH group of EPO.[33]

In our pharmacophore model for DDM and EPO-A (Figure 4C), the C15–C18 portion of the side chain of EPO-A overlaps with the C8–C15 segment of DDM, which contains

penetrates the hydrophobic cleft formed by the H6 helix and the N-terminal part of the H7 helix. EPO does not occupy this pocket,[11] while taxol places the C2 benzoyl side chain in it. Such structural differences could be partially responsible for the different morphology of MTs formed in the presence of EPO or DDM.

In conclusion, we have determined the bioactive conformation of DDM in solution from NMR tr-NOE data and found that DDM binds to tubulin in a compact globular shape. This result supports the existence of common structural requirements for the diverse natural products binding to the taxane binding pocket, with the bioactive structural motif being centered on a compact core.

With the help of both protein-mediated interligand NOE signals between DDM and EPO and the SAR data available for the two drugs, we propose a common pharmacophore model in which the C20–C24 segment of DDM does not overlap with the thiazole side chain of EPO. Similarities and differences in the pharmacophore of the two drugs may provide a rationale for the analogous but not fully equivalent biological activity of the two natural products.

Experimental Section

Tubulin preparation: Tubulin extracted from bovine brain was purchased from Cytoskeleton Inc. (Denver, CO, USA). Tubulin solution (66 µL) were diluted in buffer (350 µL, aqueous solution containing 1.5 mM phosphate, 1.5 mM calcium, and sodium at pH 7.0) and dialyzed twice with buffer (2 × 1.5 L) at 4°C. The solution was dialyzed further with D_2O buffer (2 × 15 mL) to exchange H_2O for D_2O.

Sample preparation: DDM was first dissolved in [D6]DMSO (25 µL) and then added to the tubulin solution to give a volume of 500 µL containing 5% v/v [D6]DMSO with the desired amount of ligand (0.5 mM). A final concentration of tubulin of 10 µM is estimated. 5% [D6]DMSO was used as cosolvent to increase the DDM solubility. In our experience, this small amount of DMSO does not affect either the observation or the size of tr-NOE of other tubulin ligands, such as EPO-A or taxol.

NMR spectroscopy: NMR experiments were measured on a Bruker 800 MHz spectrometer. Resonances of DDM were assigned from COSY, TOCSY, HSQC, and HMBC spectra. A series of NOESY experiments was recorded at 25°C with mixing times of 20, 40, 60, 80, 150, and 200 ms on the two samples tubulin–DDM and free-DDM. Processed spectra were analyzed with FELIX (Accelrys Software Inc., CA, USA).

Structure calculation: Structures were calculated with XPLOR-NIH 2.13[36] using restrained simulated annealing (SA) from a single extended starting template. NOE signals were used in the full relaxation matrix approach. Protocol details are provided in the Supporting Information.

Interligand NOE signals: Protein-mediated interligand NOE signals between EPO-A and DDM were observed in a NOESY spectrum acquired at 900 MHz on a sample containing 12 µM tubulin, 500 µM EPO-A, and 70 µM DDM in a D_2O/DMSO (95/5) solution. The mixing time was 300 ms.

[1] R. J. Kowalski, P. Giannakakou, S. P. Gunasekera, R. E. Longley, B. W. Day, E. Hamel, *Mol. Pharmacol.* **1997**, *52*, 613–622.
[2] S. Kar, G. J. Florence, I. Paterson, L. A. Amos, *FEBS Lett.* **2003**, *539*, 34–36.
[3] G. S. Huang, L. Lopez-Barcons, B. S. Freeze, A. B. Smith, G. L. Goldberg, S. B. Horwitz, H. M. McDaid, *Clin. Cancer Res.* **2006**, *12*, 298–304.
[4] D. M. Bollag, *Expert Opin. Invest. Drugs* **1997**, *6*, 867–873.
[5] E. Hamel, *Med. Res. Rev.* **1996**, *16*, 207–231.
[6] J. Verweij, M. Clavel, B. Chevalier, *Ann. Onc.* **1994**, *5*, 495–505.
[7] L. A. Martello, M. J. LaMarche, L. F. He, T. J. Beauchamp, A. B. Smith, S. B. Horwitz, *Chem. Biol.* **2001**, *8*, 843–855.
[8] K. H. Altmann, *Curr. Opin. Chem. Biol.* **2001**, *5*, 424–431.
[9] J. Jimenez-Barbero, F. Amat-Guerri, J. P. Snyder, *Curr. Med. Chem.: Anti-Cancer Agents* **2002**, *2*, 91–122.
[10] E. Nogales, S. G. Wolf, K. H. Downing, *Nature* **1998**, *393*, 191–191.
[11] J. H. Nettles, H. L. Li, B. Cornett, J. M. Krahn, J. P. Snyder, K. H. Downing, *Science* **2004**, *305*, 866–869.
[12] T. Carlomagno, M. J. J. Blommers, J. Meiler, W. Jahnke, T. Schupp, F. Petersen, D. Schinzer, K. H. Altmann, C. Griesinger, *Angew. Chem.* **2003**, *115*, 2619–2621; *Angew. Chem. Int. Ed.* **2003**, *42*, 2511–2515.
[13] T. Carlomagno, V. M. Sanchez, M. J. J. Blommers, C. Griesinger, *Angew. Chem.* **2003**, *115*, 2615–2519; *Angew. Chem. Int. Ed.* **2003**, *42*, 2515–2517.
[14] A. B. Smith, M. J. LaMarche, M. Falcone-Hindley, *Org. Lett.* **2001**, *3*, 695–698.
[15] E. Monteagudo, D. O. Cicero, B. Cornett, D. C. Myles, J. P. Snyder, *J. Am. Chem. Soc.* **2001**, *123*, 6929–6930.
[16] S. P. Gunasekera, M. Gunasekera, R. E. Longley, *J. Org. Chem.* **1990**, *55*, 4912–4915.
[17] V. M. Sanchez-Pedregal, M. Reese, J. Meiler, M. J. J. Blommers, C. Griesinger, T. Carlomagno, *Angew. Chem.* **2005**, *117*, 4244–4247; *Angew. Chem. Int. Ed.* **2005**, *44*, 4172–4175.
[18] F. Solomon, *Biochemistry* **1977**, *16*, 358–363.
[19] J. F. Diaz, J. M. Andreu, *Biochemistry* **1993**, *32*, 2747–2755.
[20] H. W. Wang, E. Nogales, *Nature* **2005**, *435*, 911–915.
[21] R. M. Buey, I. Barasoain, E. Jackson, A. Meyer, P. Giannakakou, I. Paterson, S. Mooberry, J. M. Andreu, J. F. Diaz, *Chem. Biol.* **2005**, *12*, 1269–1279.
[22] F. Ni, *Prog. Nucl. Magn. Reson. Spectrosc.* **1994**, *26*, 517–606.
[23] L. F. He, G. A. Orr, S. B. Horwitz, *Drug Discovery Today* **2001**, *6*, 1153–1164.
[24] P. Ballone, M. Marchi, *J. Phys. Chem. A* **1999**, *103*, 3097–3102.
[25] I. Paterson, R. Britton, O. Delgado, A. Meyer, K. G. Poullennec, *Angew. Chem.* **2004**, *116*, 4729–4733; *Angew. Chem. Int. Ed.* **2004**, *43*, 4629–4633.
[26] S. P. Gunasekera, S. J. Mickel, R. Daeffler, D. Niederer, A. E. Wright, P. Linley, T. Pitts, *J. Nat. Prod.* **2004**, *67*, 749–756.
[27] S. P. Gunasekera, G. K. Paul, R. E. Longley, R. A. Isbrucker, S. A. Pomponi, *J. Nat. Prod.* **2002**, *65*, 1643–1648.
[28] N. Choy, Y. S. Shin, P. Q. Nguyen, D. P. Curran, R. Balachandran, C. Madiraju, B. W. Day, *J. Med. Chem.* **2003**, *46*, 2846–2864.
[29] D. T. Hung, J. B. Nerenberg, S. L. Schreiber, *J. Am. Chem. Soc.* **1996**, *118*, 11054–11080.
[30] S. J. Shaw, K. F. Sundermann, M. A. Burlingame, D. C. Myles, B. S. Freeze, M. Xian, I. Brouard, A. B. Smith, *J. Am. Chem. Soc.* **2005**, *127*, 6532–6533.
[31] J. M. Minguez, S. Y. Kim, K. A. Giuliano, R. Balachandran, C. Madiraju, B. W. Day, D. P. Curran, *Bioorg. Med. Chem.* **2003**, *11*, 3335–3357.
[32] A. B. Smith, S. B. Freeze, M. J. LaMarche, T. Hirose, I. Brouard, M. Xian, K. F. Sundermann, S. J. Shaw, M. A. Burlingame, S. B. Horwitz, D. C. Myles, *Org. Lett.* **2005**, *7*, 315–318.

[33] K. C. Nicolaou, F. Roschangar, D. Vourloumis, *Angew. Chem.* **1998**, *110*, 2120–2153; *Angew. Chem. Int. Ed.* **1998**, *37*, 2015–2045.

[34] A. B. Smith, M. Xian, *Org. Lett.* **2005**, *7*, 5229–5232.

[35] I. Ojima, S. Chakravarty, T. Inoue, S. N. Lin, L. F. He, S. B. Horwitz, S. D. Kuduk, S. J. Danishefsky, *Proc. Natl. Acad. Sci. USA* **1999**, *96*, 4256–4261.

[36] C. D. Schwieters, J. J. Kuszewski, N. Tjandra, G. M. Clore, *J. Magn. Reson.* **2003**, *160*, 65–73.

[37] R. Koradi, M. Billeter, K. Wüthrich, *J. Mol. Graphics* **1996**, *14*, 51–55.